Solar Energy Materials & Solar Cells 95 (2011) 3256–3261

Contents lists available at ScienceDirect

Solar Energy Materials & Solar Cells

journal homepage: www.elsevier.com/locate/solmat

Organic photovoltaics for low light applications

Roland Steim [a,*,1], Tayebeh Ameri [**,e,1], Pavel Schilinsky [a], Christoph Waldauf [c], Gilles Dennler [d], Markus Scharber [b], Christoph J. Brabec [e,f]

[a] Konarka Technologies GmbH, Landgrabenstr. 94, D-90443 Nürnberg, Germany
[b] Konarka Technologies GmbH, Altenbergerstrasse 69, A-4040 Linz, Austria
[c] Crystalsol GmbH, Simmeringer Hauptstrasse 24, 110 Wein, Austria
[d] Konarka Technologies Inc., 116 John Street, Lowell, MA 01852, USA
[e] i-MEET; Institute Materials for electronics and energy technology, Friedrich-Alexander-Universität Erlangen-Nürnberg, Marteusstrasse 7, D-91058 Erlangen, Germany
[f] ZAE Bavaria, Am Weichselgarten 7, D-91058 Erlangen, Germany

ARTICLE INFO

Article history:
Received 28 February 2011
Received in revised form
6 July 2011
Accepted 11 July 2011
Available online 8 September 2011

Keywords:
Organic photovoltaics
Low light
Indoor
Shunt resistance
OPV
Simulation

ABSTRACT

Here we report on organic photovoltaic's (OPV) suitable for low light applications. In this paper, we illustrate the impact of R_s and R_p for indoor and outdoor applications. In addition, we propose a simple physics approach to predict the behavior of organic solar cells under various illumination intensities through electrical modeling. The combination of simulation and modeling allows to define a set of design rules for OPVs under low light illumination. The performance of various organic solar cells under low light intensity is compared with our predictions and excellent correlation is found. OPV shows high performance under low light conditions.

1. Introduction

Organic photovoltaics (OPV) are a promising candidate to solve future energy supply scenarios due to the low production costs, flexibility and the roll-to-roll printing methods [1–4]. Efficiency and lifetime of OPV is continuously increasing and made this technology more and more attractive over the last few years. OPV cells are primarily evaluated as well as certified for outdoor applications and hero efficiencies are reported for illumination at 1 sun [5–7]. Standardized tests and evaluations for indoor applications are missing although the requirements for indoor and outdoor applications are different. Since OPV enters the market for indoor and outdoor applications, they have to be optimized for indoor applications as well.

The fundamental difference between indoor and outdoor applications is the spectrum of the light source and the light intensity. For outdoor applications the reference spectrum is the AM1.5G spectrum of the sun, for indoor applications a reference light source is missing. Artificial light sources, e.g. fluorescent lamps, LEDs and incandescent lamps, are used for indoor applications. Fluorescent lamps are widely used for offices. The phosphor layer of the fluorescent lamp converts UV radiation into visible radiation. The spectrum of fluorescent lamps varies depending on the fluorescent materials used and is significantly different to the AM1.5G spectrum of the sun. The illuminance of a fluorescent lamp is measured in lx and is weighted by the sensitivity of the human eye. Typical values of the illuminance requirements for offices range between 200 and 1000 lx, which is a factor 100–500 lower than 1 sun illumination.

An ideal solar cell may be modeled by a current source in parallel with a diode; in practice no solar cell is ideal, so a shunt resistance and a series resistance component need to be added to the replacement circuit [8]. The current source represents the photocurrent I_{ph} generated within the illuminated cell. The series resistance R_s includes the ohmic contributions of the electrodes, the contact between the organic semiconductor and the metal, and the resistivity of the active materials. This resistance has to be minimized for maximum solar cell efficiency. The shunt resistance R_p illustrates the potential leakage current through the device. R_p has to be maximized to reach high efficient cells. The equivalent circuit is depicted in Fig. 1.

Based on this model the current balance of this circuit can be written as

$$I - I_0^* \left(\exp\left(\frac{e^*(V - I^* R_S)}{n^* k_B^* T} \right) - 1 \right) - \frac{V - I^* R_S}{R_P} - I_{ph} = 0 \quad (1)$$

* Corresponding author.
** Corresponding author.
E-mail addresses: rsteim@konarka.com (R. Steim), tayebeh.ameri@ww.uni-erlangen.de (T. Ameri).
[1] Both authors contribute to the same parts to the paper.

0927-0248/$ - see front matter © 2011 Elsevier B.V. All rights reserved.
doi:10.1016/j.solmat.2011.07.011

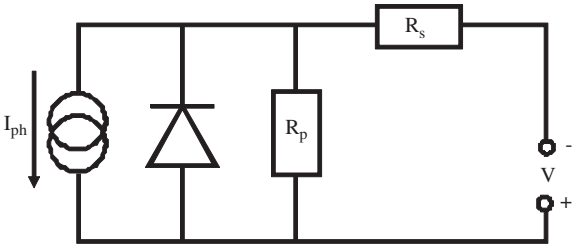

Fig. 1. Equivalent circuit of a solar cell.

where I is the current, I_0 is the saturation current, k_B is the Boltzmann constant, T is the temperature, V is the externally applied voltage, e is the elementary charge and n is the ideality factor of the diode [8]. For sufficiently high R_p the current through the shunt resistance can be neglected and V_{oc} (I=0) can be written as

$$V_{oc} = \frac{n^* k_B^* T^*}{e} \ln\left(\frac{I_{ph}}{I_0} + 1\right) \sim \ln(I_{ph}) \quad (2)$$

V_{oc} shows a logarithmic dependence on the photogenerated current. It has been shown that J_{sc} correlates linearly with the light intensity [9,10]. Thus, V_{oc} is proportional to the logarithm of the light intensity.

In this paper, we will illustrate the impact of R_s and R_p for indoor and outdoor applications by numerical simulation. In addition, we propose a simple engineering approach to predict the behavior of organic solar cells under any illumination intensity through electrical modeling. Finally, to confirm the precision of our model, we present the measured performance of various organic solar cells under low light intensities and compare them with our prediction.

2. Experimental section

All solar cells investigated were prepared on 10 Ω/square indium tin oxide (ITO) coated PET foil. These PET/ITO substrates were cleaned in an ultrasonic bath with acetone and isopropanol, followed by UV activation. On top of the PET/ITO substrates a 10 nm sol–gel processed TiO_x layer was deposited as reported earlier [11]. Then a blend of poly (3-hexyltiophene) (P3HT) and C60 derivative, 1-(3-methoxycarbonyl) propyl-1-phenyl[6,6]C_{61} (PCBM) with a mass ratio 1:0.8 from ortho-xylene (o-xylene) was coated by the same technique (about 250 nm thickness) as the active layer. A conductive layer of poly (3,4- ethylene dioxythiophene) doped with poly (styrene sulfonate) (PEDOT:PSS), diluted in isopropanol, was coated on top of active layer as the hole injection layer. Before silver deposition, devices were annealed 5 min at 140 °C. These devices were finished by the evaporation of 500 nm of silver as the top electrode. Details on the requirements for measuring efficiency and stability values can be found in Ref. [12].

The current density–voltage (J–V) characteristics of the devices were measured with a source measurement unit SMU 2400 from Keithley. For illumination at 1 sun a calibrated solar simulator (Steuernagel) is used providing a homogeneous AM1.5G spectra at 100 mW/cm^2. Since the spectrum of the metal halogen lamps of the solar simulator does not fully match with the spectrum of the sun the solar simulator is cross-calibrated by external quantum efficiency measurements. At low light condition, the OPV cells were measured with a fluorescent bulb with the light color 830. The spectrum of a fluorescent lamp and the AM1.5G spectrum of the sun in comparison to the absorption of P3HT:PCBM are shown in Fig. 2. All measurements are done in atmosphere.

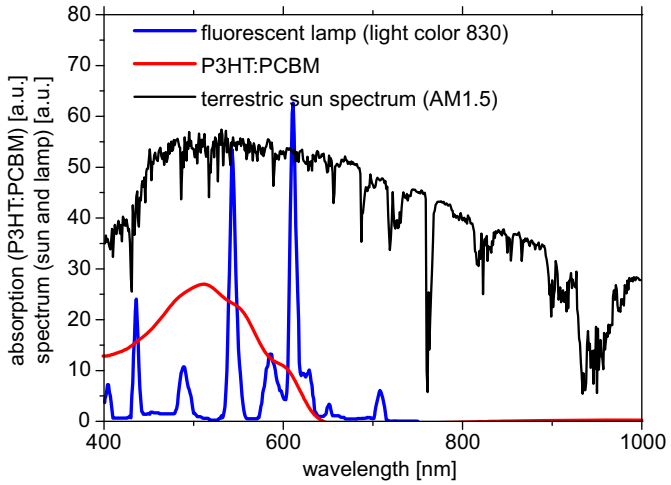

Fig. 2. Comparison of the AM1.5 spectrum of the sun and the spectrum of a fluorescent lamp with the absorption of P3HT:PCBM. The fluorescent lamp has the light color of 830 and is weighted by the sensitivity of the human eye.

3. Results and discussion

3.1. Experimental results

In the following we investigate the impact of the shunt and the serial resistance on the performance of an OPV cell. We measured the J–V characteristics of the same OPV cell at 1 sun and at 1000 lx. The impact of the serial resistance is investigated by numerically adding a series resistance Rs of 10, 25 and 50 Ω cm^2 for an otherwise experimentally measured J–V curve. Fig. 3(a) and (d) present results under 1 sun, respectively, under 1000 lx. For 1 sun illumination, the performance of the OPV cell is strongly FF limited due to the large series resistance. In addition, for high R_s values J_{sc} also becomes affected. For the measurement at 1000 lx the impact of R_s to the device performance is negligible. Obviously, Rs is rather irrelevant at these low current densities. The impact of R_p is investigated by addition of a shunt resistance of 20, 10 and 5 kΩ cm^2. These values of R_p do not limit the performance of the OPV cell under 1 sun illumination (Fig. 3b). However, under indoor low light conditions, the FF is significantly affected by adding R_p. Lower R_p values even affect V_{oc}. Summarizing these initial findings, the impact of the shunt and serial resistance is different for indoor and outdoor applications. Low light applications require high shunt resistances to guarantee full performance. Outdoor applications can handle a lower shunt resistance, but are more sensitive to large Rs values. Next, we will investigate the impact of the shunt on the solar cell performance, the V_{oc} and FF of various P3HT:PCBM solar cells with different shunt resistances.

Four different cells with shunt resistances of 85, 40, 20 and 800 Ω cm^2 were chosen. The R_p value was calculated from the slope of the J–V curve at 0 V between the points—0.1 and 0.1 V. Illumination with 5000, 1000 and 500 lx was provided from a fluorescent lamp, for 100,000 lx illumination a metal halogen bulb was used, which corresponds roughly to 1 sun. The power output, V_{oc} and FF are shown in Fig. 4. At 100,000 lx the measured cell performance is comparable for all investigated cells. The power output of the organic solar cells at MPP is 2.5 mW/cm^2 ± 10%, FF of 55% ± 10% and V_{oc} of 550 mV ± 10% under 100,000 lx illumination. For low light intensities the situation is completely different. OPV cells with comparable performance at 100,000 lx show a variation from 1.3 to 19 μW/cm^2 at 1000 lx. The organic solar cell with the highest shunt resistance has the highest power output; the cell with lowest shunt resistance has the lowest power

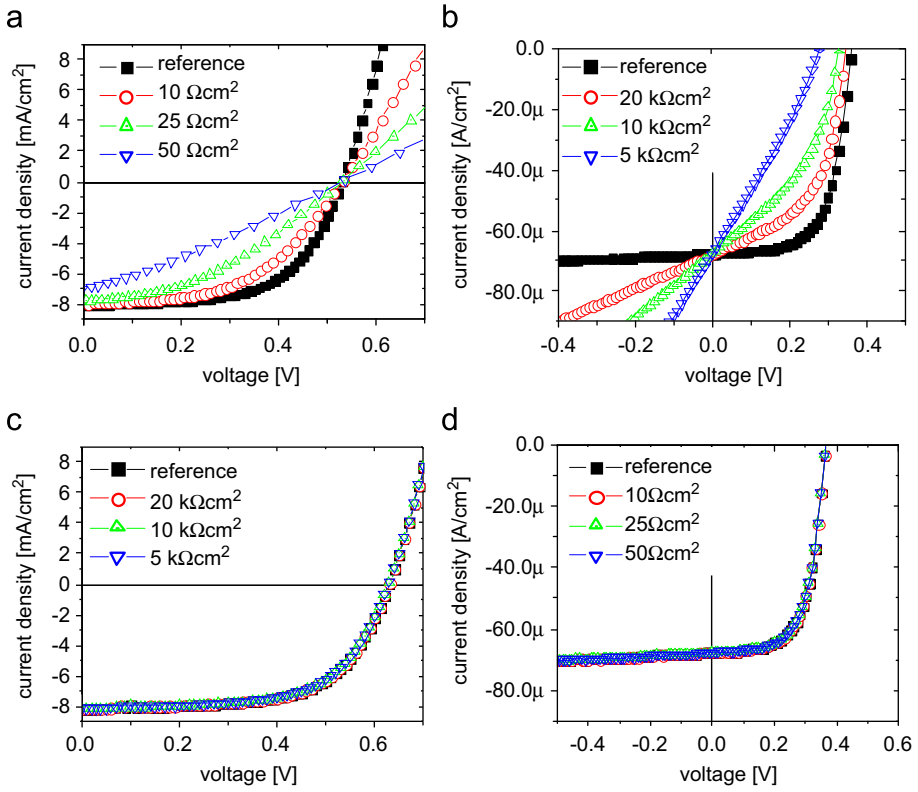

Fig. 3. Illustration of the impact of R_p and R_s to the J–V characteristics of OPV cells measured at 1 sun and 1000 lx. R_s and R_p are numerically included into to the measured J–V characteristic of the reference OPV cell. (a) 1 sun, Rs variation, (b) 1 sun, Rp variation, (c) 1000 lx, Rp variation and (d) 1000 lx, Rs variation.

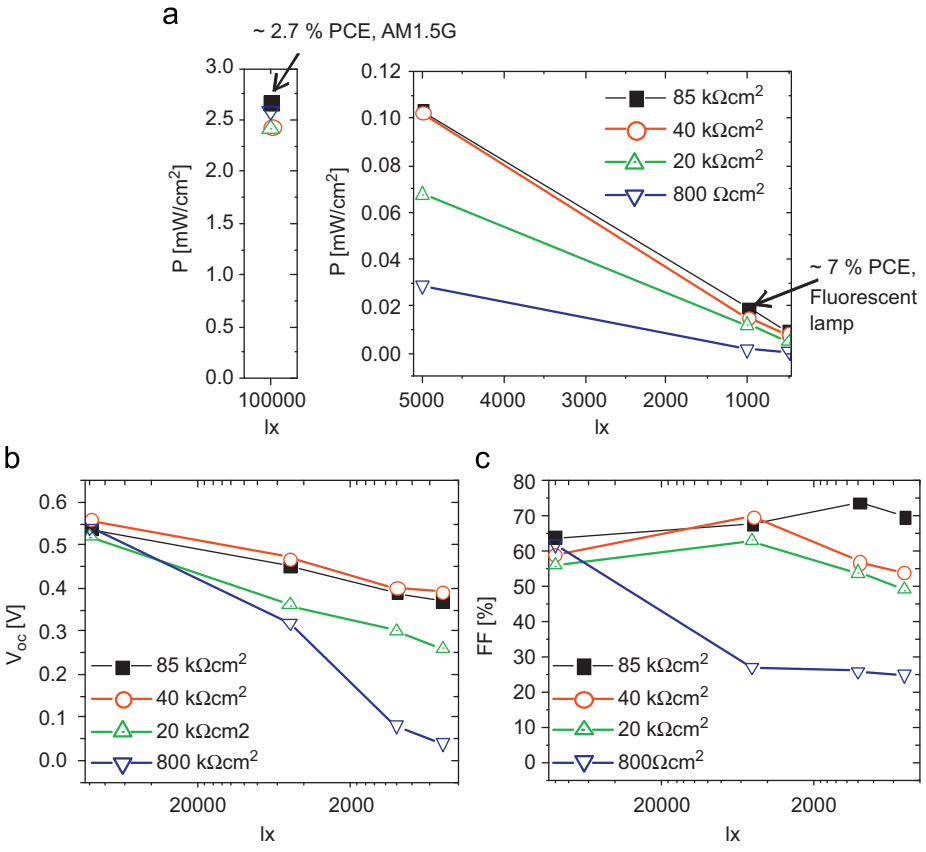

Fig. 4. Impact of R_p to the (a) power output, (b) V_{oc} and (c) FF of OPV cells. OPV cells with varying R_p are measured at light intensities of 100,000, 5,000, 1,000 and 500 lx.

output. The situation is similar at 5000 and 500 lx. The FF of the cells with a shunt resistance of 800 Ω cm^2 decreases with decreasing light intensity. Contrarily, for a higher shunt resistance the FF increases with decreasing light intensity due to reduced impact of R_s and can reach a maximum. The FF of the OPV cell with a shunt resistance of 40 kΩ cm^2 increases from 60% at 100,000 lx to 70% at 5000 lx. The organic solar cell with the highest shunt resistance of 80 kΩ cm^2 shows an improvement of the FF from 64% measured at 100,000 lx to 74% measured at 1000 lx. A further reduction of the light intensity below 1000 lx again leads to a drop in FF. With increasing shunt resistances, the maximum FF shifts to lower light intensities. All cells in common are a decrease of V_{oc} with decreasing light intensity. OPV cells with lower R_p show a larger drop in V_{oc}. We determined the low light efficiency of the investigated cells by a fluorescent lamp (Philips F32T8/TL830). The illumination intensity of the lamp was determined with a pyranometer (Eppley model PSP) and 1000 lx were found to be equal 0.27 mW/cm^2. The best presented cell has an electrical power output of 19 μW/cm^2 under 1000 lx. This corresponds to an efficiency of 7%.

Interestingly we obtained similar results when the illuminated area of an OPV cell with a high shunt resistance (around 100 kΩ cm^2) is reduced with the help of a shadow mask. We reduced the active area of a solar cell sized 1 cm^2 from 1 cm^2 to 0.7 mm^2 and measured J–V characteristics with different sized rectangle masks. The measured parameters are presented in Fig. 5. As it is expected, the J_{sc} is approximately constant with the illuminated area. The V_{oc} versus the active area shows a linear behavior in the semi-logarithmic scale. The FF is increasing from 0.6 at 1 cm^2 to 0.66 at a particular area of 15.55 mm^2. When the active area is getting smaller than 4 mm^2, the FF is dropping again to only 0.55 at 0.7 mm^2. The same trend of FF alterations is shown in Fig. 4(c) when the illuminated light intensity is reduced. Chu et al. also have reported the same effect of low light intensity on I_{sc}, V_{oc} and FF changes [13].

Overall, these findings imply that the relatively relaxed requirements for R_s open up the possibility to use alternative transparent electrode materials for low light applications. Even a lowest cost alternative like PEDOT:PSS is a promising material, which would provide sufficient conductivity as electrode for indoor applications.

3.2. Simulation

We propose a simple engineering approach to predict the light intensity behavior of solar cells. This prediction requires only two inputs, namely i) the J–V characteristic of the device in the dark and ii) the J–V characteristics of the device under a known light intensity. The principle of the modeling is explained in more details in Ref. [14]. Since J_{sc} is directly proportional to the light intensity, it is straight to predict it over several orders of magnitude versus the light intensity. For a complete prediction of the device performance under different light intensities, one also needs the relation of the FF and the V_{oc} versus the light intensity. This relation can be derived from an analysis of the dark J–V characteristics. The J–V characteristics of a photovoltaic device in the dark usually consist of 3 distinctive parts, which are easily identified in a semi-logarithmic plot shown in Fig. 6:

- A linear dependence of the current on the voltage at low and negative voltages (red part in Fig. 6)—the shunt regime.
- An exponential part at intermediate voltages (green part in Fig. 6)—the diode regime.
- Another linear regime at high voltages (blue part in Fig. 6)—the series regime.

Our main assumption is that the dark diode characteristics are not getting changed under illumination [11].

The open circuit voltage of a photovoltaic device represents the voltage at which the current generated by the light equals the dark current. Thus the open circuit voltage follows directly the dark curve behavior: It drops logarithmically where the generated current is within the exponential regime and it decreases linearly at lower currents in the shunt regime. With that, V_{oc} can be directly calculated from the dark J–V curve as a function of the light intensity. Fig. 7 shows the calculated V_{oc} versus the light intensity for a large range of shunt resistance. The light intensities are presented as a fraction of 1 sun (fraction of 100 mW/cm^2 AM1.5G). When the shunt resistance of the device is as small as 2000 Ω cm^2, a sharp drop of the V_{oc} is observed at intensities less than 1/10th of the sun. This trend is repeated for other low shunt resistance. According to our simulation, a shunt resistance in the order of 100 kΩ cm^2 is required to ensure the

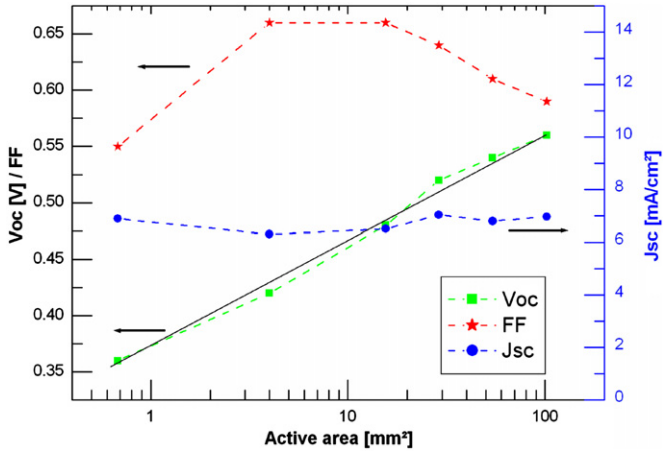

Fig. 5. Measured parameters of a P3HT:PCBM solar cell of active area of 1 cm^2 versus the actual size of illuminated area.

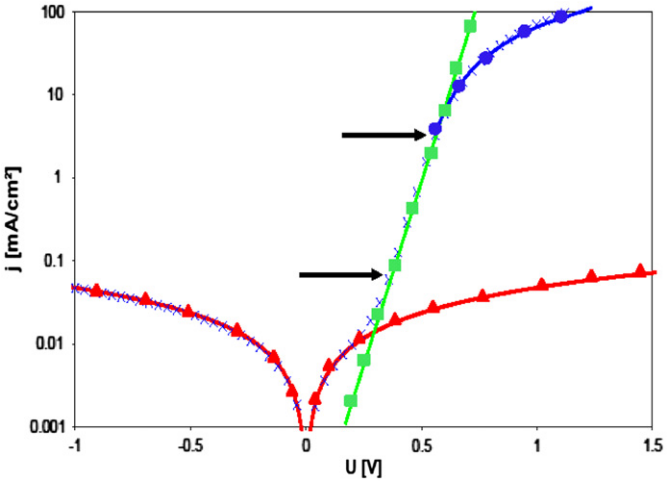

Fig. 6. Measured dark curve of a representative photovoltaic device (x curve) with the indication of the different voltage regimes concerning the relation of current and voltage: the red triangle part indicates a linear regime at low voltages corresponding to parallel resistance, the green square part indicates the exponential increase and, thus, the diode behavior, and the blue circle part is another linear part at higher voltages corresponding to series resistance. In between the bottom and the top arrow the device behaves like an ideal photodiode. Below the bottom arrow V_{oc} and FF is affected by losses through the shunt and above the top arrow J_{sc} and FF are reduced by the series resistance. (For interpretation of the references to color in this figure legend, the reader is referred to the web version of this article).

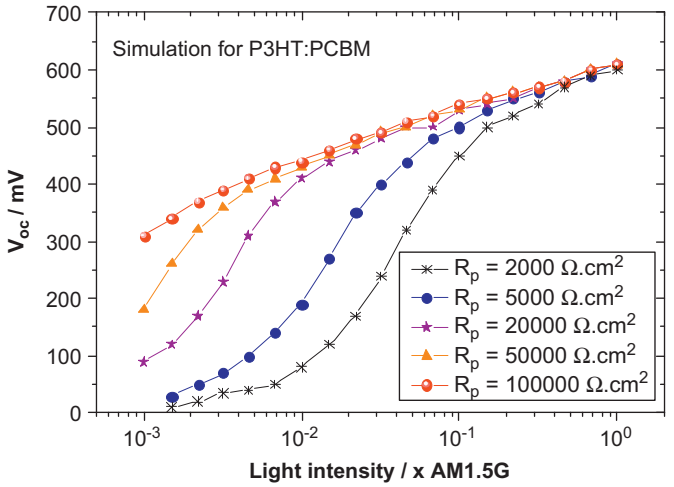

Fig. 7. Calculated V_{oc} (by our electrical modeling) versus the light intensity for different shunt resistance of a P3HT:PCBM solar cell.

full V_{oc} of P3HT:PCBM devices under low light intensities. This finding is confirmed by our experimental results.

For the FF a similar consideration can be made: The FF is suffering from series resistance losses where the generated current is within the linear regime at high voltage; while the FF gains its maximum amount when the generated current hits exponential regime and stays constant over the whole exponential regime (between top and bottom arrows in Fig. 6). Below this regime where the generated current is within the second linear regime at low voltages, the FF drops again due to shunt losses.

This allows the rough prediction that the efficiency of any device is maximal when the photogenerated current hits the highest point in the exponential regime, just before the upper linear regime (top arrow in Fig. 6). Below this point, the efficiency drops in a logarithmic manner versus the light intensity, since the FF remains constant and the V_{oc} follows a logarithmic decay. Finally, when the light generated current is within the shunt region (bottom arrow in Fig. 6), the V_{oc} starts to drop linearly and the FF evolves to the minimal value of 25%.

To confirm our model predictions, we compared the outdoor low light performance of different P3HT:PCBM solar cells with the prediction. The light spectrum here is the one of the sun. Fig. 8(a) shows the *J–V* characteristic of a device with a 500 nm thick active layer in the dark and under 1 sun illumination. A device with such a thick semiconductor layer already has a non-negligible serial resistance. This large series resistance causes a bias loss at photocurrent densities as low as app. 0.5 mA/cm^2. This loss is seen as a deviation from the exponential slope and reduced the FF already at ~1/20th of a sun. On the other hand, there are no FF losses when going down to even very outdoor low light intensities (down to 1/5000th of the sun) due to the high shunt resistance. Therefore this thick device will have a reasonable good low light device performance, but suffer from losses at 1 sun operation. Fig. 8(b) summarizes the light intensity measurements (done with gray filters). As predicted, the maximum efficiency of around 2.8% is reached at roughly 1/20th of a sun.

The same procedure is run for a device with a 200 nm thin P3HT:PCBM active layer. Series resistance limitations are not an issue here and this clearly reflected by the *J–V* characteristic of this device shown in Fig. 8(c). The deviation from the exponential slope occurs at current densities of app. 2–3 mA/cm^2, which is the equivalent photocurrent under app. 1/5th of the sun. However, the leakage current (shunt) of this device is much higher than the previous one, and this impacts the low light intensity performance as seen from the experimental data shown in Fig. 8(d). Further, Fig. 8(d) shows that the FF breaks down at light intensities less that 1/100th sun. This is an equivalent photocurrent of app. 0.1 mA/cm^2. Again, the deviation from the exponential part occurs at these current densities, bringing the experimental data in excellent agreement with the model. In contrast to the thick device, this thin device has the highest performance of 2.7% under just 1/5th of the sun intensity.

For integration of OPV into products the serial interconnection of several cells to modules is necessary. OPV modules with 10 cells circuited in series are investigated and it is found that modules with a high R_p of each individual cell show good low light performance since the module *V* is the superposition of the *V* of the individual cells. One application for OPV is the integration to cordless low electrical power consuming products, e.g. sensors, alarms, remote access controls and small LCD displays. Dennler et al. summarized the energy consumption of several cordless consumer products in the μWh to low mWh range per day and also discussed the energy storage in batteries [15]. An OPV module of a few cm^2 is sufficient to provide the energy needed.

But also for integrating OPV in the facade of buildings or in mobile chargers [16] a good low light performance is beneficial since the alignment of the module to the sun is not always ideal, e.g. when the facade is facing north. The overall energy production per day is the integration over the full day, including clouds reducing the light intensity and the dawn for which the good low light performance of OPV is beneficial.

4. Conclusion

In this paper we investigated the impact of the shunt and serial resistance on the performance of OPV cells under indoor and outdoor conditions. We showed that a high shunt resistance is essential for indoor, i.e. low light applications whereas R_s is less critical. The situation is exactly opposite for outdoor applications. For indoor applications (1000 lx) a shunt resistance of 85 k Ω cm^2 or higher and a serial resistance of 50 Ω cm^2 or lower is required. For outdoor applications at 1 sun a shunt resistance of 1 k Ω cm^2 or higher is sufficient and a serial resistance of 3 Ω cm^2 or lower is required to prevent losses. OPV cells, which are operated in both, indoor and outdoor illumination require a shunt resistance of 85 k Ω cm^2 or higher and a serial resistance of 3 Ω cm^2 or lower.

Analysis of the *J–V* curves and a simple fitting of the exponential part of the *J–V* curve show that the device efficiency is highest just before the series resistance losses start. This is seen by a deviation from the exponential slope at high current conditions. (top arrow in Fig. 6). At this very point, the open circuit voltage is highest while the FF is not yet reduced. Below this point, the efficiency drops logarithmically with the light intensity, since the FF remains constant and the V_{oc} follows a logarithmic decay. Finally, when the light generated current is in the order of the shunt current (bottom arrow in Fig. 6), the V_{oc} starts to drop linearly and the FF evolves towards the minimal value of 25%.

For low light applications, the impact of the serial resistance is not that dramatic, and novel transparent electrode materials may become feasible. This suggests replacing the expensive ITO by inexpensive conductor, such as PEDOT:PSS [17]. For outdoor applications highly conductive electrode materials remains a must.

In addition, a light source with a defined spectrum for indoor applications has to be standardized. In this work, a hero efficiency of 7% under low light conditions under illumination of a fluorescent lamp with the light color 830 has been achieved.

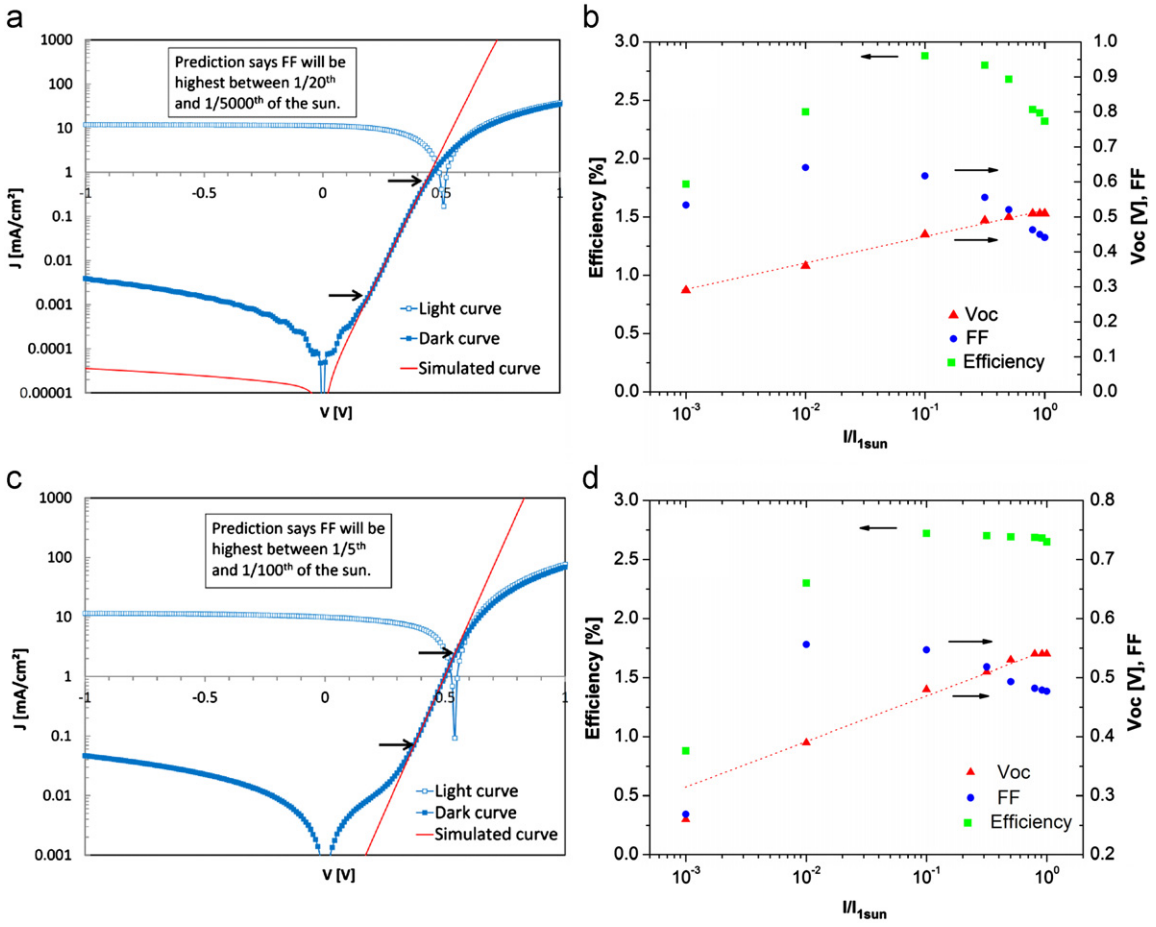

Fig. 8. Dark (closed square) and illuminated (1 sun) (open square) *J–V* data and exponential slope of the diode best fitting the device behavior (red solid curve) of a (a) thick P3HT:PCBM device (c) thin P3HT:PCBM device, and measured parameters under low light intensities for a (b) thick P3HT:PCBM device (d) thin P3HT:PCBM device (the dotted red line is a logarithmic fit to the V_{oc}).

References

[1] G. Dennler, M.C. Scharber, C.J. Brabec, Polymer-fullerene bulk-heterojunction solar cells, Adv. Mater. 21 (2009) 1323–1338.

[2] F.C. Krebs, M. Jorgensen, K. Norrman, O. Hagemann, J. Alstrup, T.D. Nielsen, J. Fyenbo, K. Larsen, J. Kristensen, A complete process for production of flexible large area polymer solar cells entirely using screen printing-first public demonstration, Sol. Energy Mater. Sol. Cells 93 (2009) 422–441.

[3] F.C. Krebs, S.A. Gevorgyan, J. Alstrup, A roll-to-roll process to flexible polymer solar cells: model studies, manufacture and operational stability studies, J. Mater. Chem. 19 (2009) 5442–5451.

[4] T.D. Nielsen, C. Cruickshank, S. Foged, J. Thorsen, F.C. Krebs, Business, market and intellectual property analysis of polymer solar cells, Sol. Energy Mater. Sol. Cells 94 (2010) 1553–1571.

[5] Y. Liang, Z. Xu, J. Xia, S.-T. Tsai, Y. Wu, G. Li, C. Ray, L. Yu, For the bright future: bulk heterojunction polymer solar cells with power conversion efficiency of 7.4%, Adv. Mater. 22 (2010) E135–E138.

[6] H.Y. Chen, J.H. Hou, S. Zhang, Y. Liang, G. Yang, Y. Yang, L. Yu, Y. Wu, G. Li, Polymer solar cells with enhanced open-circuit voltage and efficiency, Nat. Photonics 3 (2009) 649–665.

[7] S.H. Park, A. Roy, S. Beaupré, S. Cho, N. Coates, J.S. Moon, D. Moses, et al., Bulk heterojunction solar cells with internal quantum efficiency approaching 100, Nat. Photonics 3 (5) (2009) 297–302.

[8] Eduardo Lorenzo, Solar Electricity: Engineering of Photovoltaic Systems, Progensa, 8486505550, 1994.

[9] Pavel Schilinsky, Loss Analysis of the Power Conversion Efficiency of Organic Bulk Heterojunction Solar Cells, 〈http://oops.uni-oldenburg.de/frontdoor.php?source_opus=180〉.

[10] P. Schilinsky, C. Waldauf, C.J. Brabec, Recombination and loss analysis in polythiophene based bulk heterojunction photodetectors, Appl. Phys. Lett. 81 (2002) 3885–3887.

[11] C. Waldauf, M. Morana, P. Denk, P. Schilinsky, K. Coakley, S.A. Choulis, C.J. Brabec, Highly efficient inverted organic photovoltaics using solution based titanium oxide as electron selective contact, Appl. Phys. Lett. 89 (2006) 233517.

[12] M.O. Reese, S.A. Gevorgyan, M. Jørgensen, E. Bundgaard, S.R. Kurtz, D.S. Ginley, D.C. Olson, M.T. Lloyd, P. Morvillo, E.A. Katz, A. Elschner, O. Haillant, T.R. Currier, V. Shrotriya, M. Hermenau, M. Riede, K.R. Kirov, G. Trimmel, T. Rath, O. Inganäs, F. Zhang, M. Andersson, K. Tvingstedt, M.L. Cantu, D. Laird, C. McGuiness, S. Gowrisanker, M. Pannone, M. Xiao, J. Hauch, R. Steim, D.M. DeLongchamp, R. Rösch, H. Hoppe, N. Espinosa, A. Urbina, G.Y. Uzunoglu, J.B. Bonekamp, A.J.J.M.V. Breemen, C. Girotto, E. Voroshazi, F.C. Krebs, Consensus stability testing protocols for organic photovoltaic materials and devices, Sol. Energy Mater. Sol. Cells 95 (2011) 1253–1267.

[13] C. Chu, H. Yang, W. Hou, J. Huang, G. Li, Y. Yang, Control of the nanoscale crystallinity and phase separation in polymer solar cells, Appl. Phys. Lett. 92 (2008) 103306.

[14] P. Schilinsky, C. Waldauf, J. Hauch, C.J. Brabec, Simulation of light intensity dependent current characteristics of polymer solar cells, J. Appl. Phys. 95 (2004) 2816.

[15] G. Dennler, S. Bereznev, D. Fichou, K. Holl, D. Ilic, R. Koeppe, M. Krebs, A. Labouret, C. Lungenschmied, A. Marchenko, D. Meissner, E. Mellikov, J. Meot, A. Meyer, T. Meyer, H. Neugebauer, A. Opik, N.S. Sariciftci, S. Taillemite, T. Wohrle, A self-rechargeable and flexible polymer solar battery, Sol. Energy 81 (8) (2007) 947–957.

[16] F.C. Krebs, J. Fyenbo, M. Jørgensen, Product integration of compact roll-to-roll processed polymer solar cell modules: methods and manufacture using flexographic printing, slot-die coating and rotary screen printing, J. Mater. Chem. 20 (2010) 8994–9001.

[17] R. Steim, F.R. Kogler, C.J. Brabec, Interface materials of organic solar cells, J. Mater. Chem. 20 (2010) 2499.